Object-Oriented Approach for Building Footprint Extraction from High Resolution Satellite Imagery: A Comparative Study

Arshad Peer Mohamed[1] & Minakshi Kumar[1*]

[1]*Indian Institute of Remote Sensing (IIRS), Indian Space Research Organisation (ISRO), 4 Kalidas Road, Dehradun, India*

*minakshi@iirs.gov.in

Abstract: The very high resolution (VHR) satellite imagery is consistently necessary for cartographers and urban planners to identify and map crucial urban feature like different types of buildings. Building footprints are crucial dynamic elements in the planning and design of smart cities, in the creation of master plans, and in numerous other urban applications. The most challenging problem is identifying different sorts of buildings in satellite imagery since they frequently blend spectrally with other spatial characteristics. Urban buildings can be effectively extracted when very high resolution (VHR) satellite imagery (<1 m) is made available. Conventional pixel-based approaches fail to achieve high accuracy in detecting building information. Advance ML classifiers based on Object-based image classification (OBIA) are used because of their innovative paradigm and high accuracy in building extraction to reduce the limitations of traditional classifiers in handling such spectral heterogeneity in collecting building information. The main focus of this study is to demonstrate how distinct building footprints may be extracted using several classification algorithms and present the most successful one for achieving high accuracy in information detection. Given that the OBIA comprises both segmentation and classification, the multi-resolution segmentation (MRS) technique is used to group the pixels into several segments by choosing appropriate parameters for building detection, such as scale, shape, and compactness. In the study, two separate classification methods were used: sample-based methods like nearest neighbour (NN), support vector machine (SVM), and random trees (RT) and rule-based method like fuzzy membership function. The membership function and object primitives acted as the foundation for the rule set. When assigning the membership function, the GLCM Homogeneity range is used to address the main difficulty of distinguishing buildings from other features like rail tracks. The classified results underwent an area-based quantitative assessment, which revealed that the Fuzzy rule had the greatest overall accuracy percentage at 97.74%, followed by RF, NN, and SVM at 96.84%, 96.2%, and 96.12%, respectively. Completeness, correctness, and quality are the three accuracy indexes used in the object-based accuracy measure. The achieved percentages for these three accuracy indices are 88.23%, 85.71%, and 77%, respectively. The study demonstrate the significance of the approach in large scale feature extraction, which would be useful in monitoring the urban system that are of use to urban planners. Integration of this approach with geographic information system (GIS) and cartography can provide a means to find and update urban information accurately and efficiently.

Keywords: High resolution image, Object-based image analysis (OBIA), Building Footprint extraction, Multiresolution Segmentation, Image classification.

1. Introduction

Feature extraction from the high resolution satellite imageries is a crucial component of remote sensing for the creation of urban theme maps, urban planning and infrastructure, detecting changes in property management, and land use analysis [1]. In particular, detection and classification of building features in an urban landscape play a key role in the estimation of the amount of urbanization, collection of property tax, smart city planning, real estate and disaster management. The very high resolution satellite data have increased in popularity due to their high resolution, accuracy, and efficient acquisition and have been used for a variety of applications as remote sensing technology has advanced [2]. Compared to existing medium and high resolution remote sensing datasets like Landsat TM, ETM+, OLI/TIRS (30 m), Sentinel-2 (10 m), and other HR datasets, the VHR datasets from Worldview satellite provide precise information on specific objects included in an image [3]. It is evident that the precise information extraction is difficult to achieve from low and medium resolution satellite imageries. Even building footprints detection from VHRI has been challenging due to obstacles like trees, barren land, railway lines, and incomplete buildings [4]. The techniques for detecting urban feature characteristics fall into two basic categories: pixel-based and object-based classification methods [5]. Low-level characteristics are frequently extracted using a pixel-based technique. High-level characteristics are extracted using object-based image analysis (OBIA), which identifies shapes in images regardless of lighting, translation, orientation, or scale [6]. Spatial information is more crucial than spectral information for distinguishing the urban characteristics [7]. Other high resolution satellites can also extract extensive information about the objects from their images, including IKONOS, Quickbird, and GeoEye [8]. The approach known as "object-based image analysis" (OBIA) is carried out based on an object that a person can understand [9]. Image segmentation is used that divides the image into a number of clusters by altering the morphology of the objects and the multi-resolution segmentation technique is offered by eCognition software for operation [10], [11]. The classification approach is needed as a remedy to enhance segmentation [12].

According to the numerous published studies, it is clear that the extraction of different types of building footprints through OBIA in less dense urban environments [13], [14], [15] . Due to the diverse urban landscapes inherent in India and the variety of building materials, colours, textures, and complexity, it is challenging to distinguish one building from another through traditional approaches. The scene is also made more difficult and time-consuming to analyse by the inclusion of other urban features, such as roadways and railway tracks, which are the most likely pixels to be mixed with building materials. The extraction of different building footprints from VHRI data is also one of the challenges for the current scenario. Hence the study fills the gap by using OBIA approach in these difficult circumstances, together with sample-and rule-based classification techniques, is innovative and can be very beneficial for the extraction of different sorts of buildings from dense, unplanned urban areas. The study also presents the most effective approach for achieving high accuracy in feature detection after comparing the outcomes of the accuracy assessment of extracted buildings.

2. Study Area and Datasets used

The current investigation makes use of various sorts of buildings situated in the Angamally locality of Ernakulam district, Kerala, India. The region of interest covers approximately 152 hectares and is located at a Mean Sea Level (MSL) of 25 m approximately. Building structures with varying roof pitches, metal sheets, and concrete kinds make up the area, which was chosen to compare the extraction accuracy of footprint extraction. **Figure 1** below displays a map of the study area. The high resolution image was acquired from the Worldview-2 satellite and the same used in this study. The details of obtained satellite dataset are shown in the below **Table 1** and is used to create subset in accordance with the boundary of the study area. The map projection and coordinate system of the subset have been changed to EPSG: 32643 - WGS 84 / UTM zone 43N for the purpose of completing further tasks in the study. The eCognition Developer 9.2 is used for segmenting and classifying the image objects.

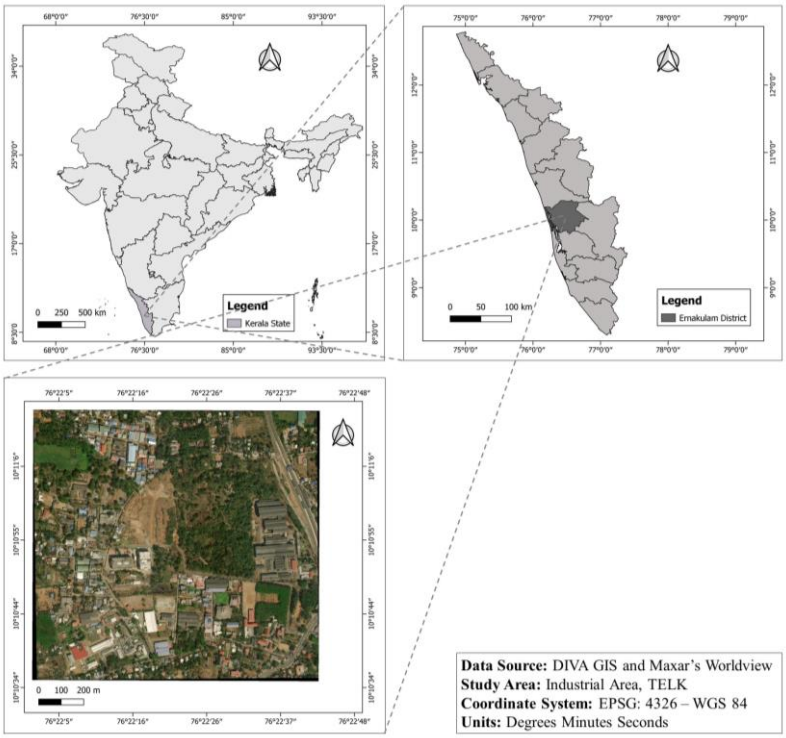

Figure 1. Study Area Map

Table 1. Details of acquired High Resolution Dataset

Satellite/ Sensor	Date of Acquisition	Spatial Resolution	Spectral Bands	Tile Number
Worldview-2	03-02-2017	0.3 m	B1 – Blue B2 – Green B3 – Red	1040010028ACAA00
Source: *Maxar's open data program open data* [16]				

3. Methodology

The general flow of methodology is shown in **Figure 2** below. The following sections go over each step's specifics in detail.

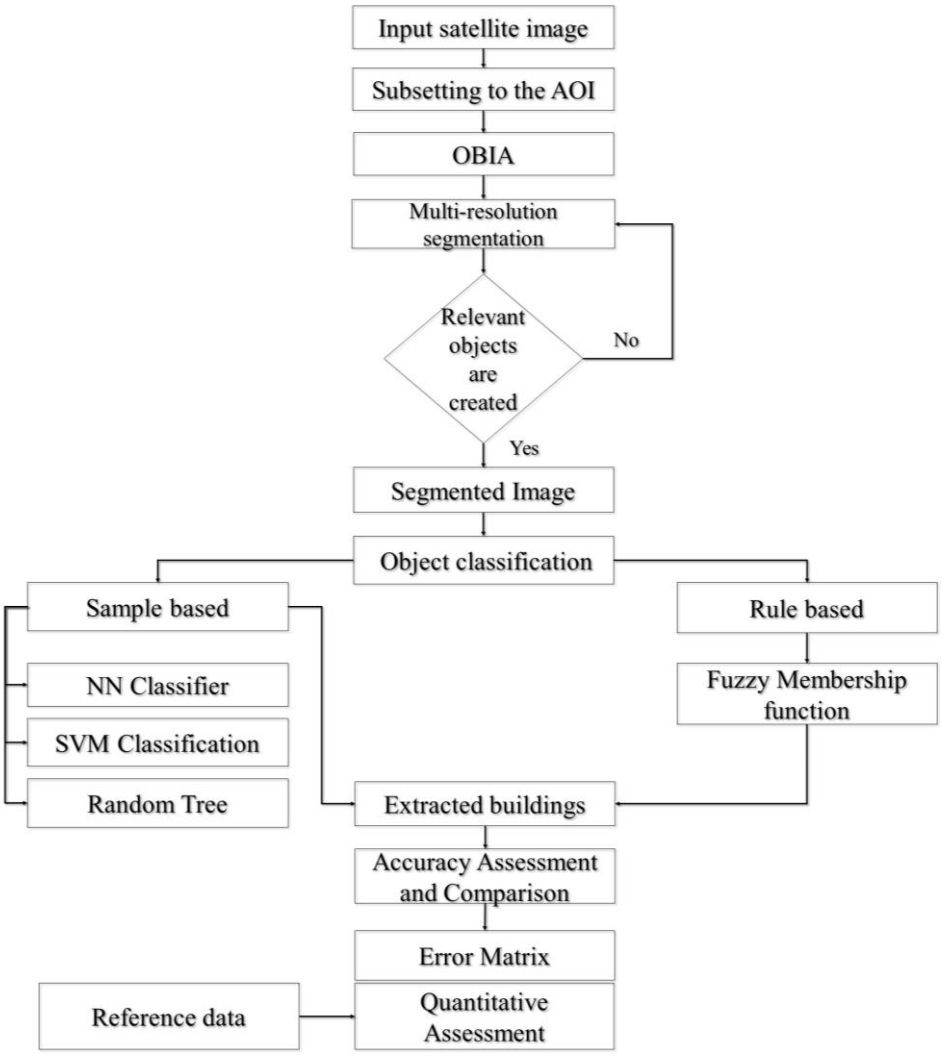

Figure 2. General Methodology

3.1. Multi-resolution Segmentation

The initial and most important process during the implementation of the OBIA technique is the image segmentation. Multi-resolution segmentation is a type of bottom-up, region-based segmentation algorithm and it is chosen in the study as it reduces average heterogeneity and improves the homogeneity of image objects [17]. **Figure 3 (a)–(d)** illustrates objects created using various segmentation parameters.

Scale, form, and compactness factor are the primary factors taken into account for the multiresolution segmentation. The scale factor is based on the amount of specificity needed for precise classification. While the shape factor modifies the spectral and spatial uniformity of objects, the compactness factor preserves the regularity and smoothness of the object boundaries [18]. Different scales, shapes, and compactness factors are evaluated for MRS. In comparison to scale 120, scale level 50 provides a higher amount of detail. The image is segmented in the OBIA process by considering four different scale, shape, and compactness factors in order to get the best, optimum segmentation parameters for further classification purposes.

3.2. Object Classification

The next critical stage in OBIA is classification of the segmented data. In this step, the objects are classified by applying the chosen supervised classifiers and rule-based classification in the study. The classification algorithms begin by taking into consideration the segmented image with a scale of 100, the shape, and the compactness factor of 0.5 and 0.7 respectively for achieving higher accuracy. In Sample based Classification, the three supervised classification algorithms such as Nearest Neighbour (NN), Support Vector Machine (SVM), and Random Forest (RF) were performed in extracting building footprints, Number of experiments were carried out by tuning the parameter for each classifier in order to optimise it.

NN is used to identify the predetermined set of training samples that are spatially closest to the new location [19]. To classify the segmented objects, a group of pixels is chosen as a training sample for each class. SVM creates a hyperplane or group of hyperplanes that can be exploited for classification [20]. The linear kernel was used in this work to show the relationships between samples from different classes. Cost (C) is a crucial tuning parameter for the linear kernel which was set to 2 by default. The random tree classifier identifies an input feature element using each tree in the forest [21]. The maximum depth, categories, and maximum number of trees were set to 20, 16, and 80, respectively after multiple iteration. The rest of the parameters settings were kept default.

In Rule based Classification, user defined rules are used, which makes use of human knowledge. The fuzzy membership function is applied in the current study as a rule set to extract buildings. It classifies the image, with each object's value falling between the ranges of 0 and 1 [22]. For the purpose of determining the classification threshold value, eCognition offers a variety of feature spaces. The homogeneity of the Grey Level Co-occurrence Matrix (GLCM), which is obtained from texture data, is employed in this work to distinguish between pixels with the same spectral reflectance. The minimum to maximum membership function of GLCM homogeneity was set as 0 to 0.23 for the non-building class and above 0.23 for the building class for the purpose of obtaining the appropriate information.

3.3. Accuracy Assessment

An essential phase in the object-based image classification process is accuracy assessment. The classification accuracy in this study was determined using an error matrix, an area-based accuracy measure, and an object-based accuracy measure. In this study, error matrix was calculated for all the classified results produced by the supervised classification approaches such as NN, SVM and RT. It is used to calculate the overall accuracy, producer accuracy, user accuracy, and kappa coefficient [23]. Two classes such as building and non-building were chosen for executing this accuracy assessment. The area-based accuracy measurements were determined as percentages for the results generated from NN, SVM, RT, and fuzzy membership function. The following set of equations were employed by referring an existing study in order to determine accuracy [24]. Additionally, for each extracted building, the proportion of difference error has been computed.

a) Percentage Accuracy = Extracted building area / Reference building area $*$ 100 ……Eq. (1)
b) Overall Accuracy = Σ Percentage accuracy of each building / Total Number of considered buildings ……Eq. (2)

In object-based accuracy evaluation, a numerical output is measured, which verifies the precision of the classification outcomes [25]. Only the detected buildings from the fuzzy based classification were subjected to this quantitative evaluation. The assessment was carried out with reference to the hands on digitized buildings. Three components, including True Positive (TP), False Positive (FP), and False Negative (FN), were discovered by comparing extracted and reference buildings [26]. These elements are utilised to accurately appraise the extracted buildings. The below mentioned equations were employed to determine the correctness percent, completeness percent, and quality percent for evaluating the accuracy of extracted buildings [27].

a) Correctness (%) = TP / TP+FP ……Eq. (3)
b) Completeness (%) = TP / TP+FN ……Eq. (4)
c) Quality (%) = TP / (TP+FP+FN) * 100 ……Eq. (5)

4. Results and Discussion

4.1. Results of Image Segmentation

In this study, the appropriate scale, shape, and compactness parameters were set as 100, 0.5, and 0.7 accordingly after testing with various values for several iterations. It is clear that image segments with the same hue factor are grouped together, and the generated image objects are of higher quality as an outcome of the shape factor. The different segmentation parameters examined are displayed in **Table 2** below.

Table 2. Different segmentation parameters used for experimentation purpose.

Parameter	Trial 1	Trial 2	Trial 3	Trial 4
Scale	50	70	100	120
Shape	0.3	0.3	0.5	0.5
Compactness	0.5	0.7	0.7	0.8

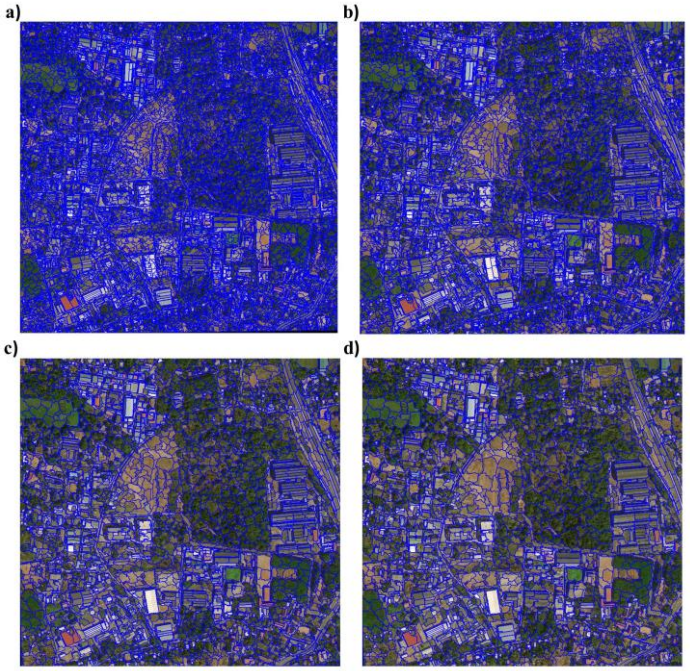

Figure 3. a) Trial 1 segments, b) Trial 2, c) Trial 3, d) Trial 4

4.2. Results of Image Classification

The standard NN classifier is applied to the features to be extracted from the image and the classified result is shown in **Figure 4 (a).** Once the cost parameter was set, the SVM-classified buildings are created and depicted the same in **Figure 4(b).** The essential RF classification parameters such as Maximum depth, Categories and number of trees were applied to produce the resulting image, as seen in **Figure 4 (c).** The removal of incorrectly classified classes is typically accomplished by using more samples for each class, and then applying the model. In rule based classification, the buildings were set apart from all other features for which GLCM homogeneity was applied using the fuzzy membership function. As per the considered threshold values, image segments are classified into buildings and non-buildings. **Figure 4 (d)** shows the classification outcome of the fuzzy rule set.

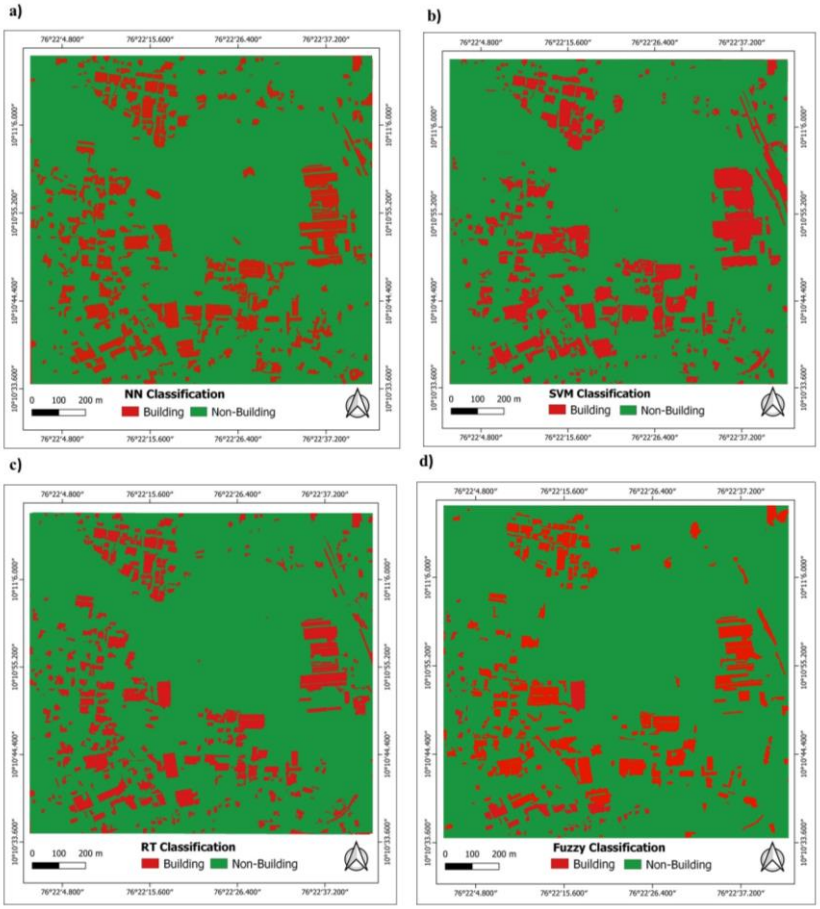

Figure 4. a) NN classified buildings, b) SVM classified buildings, c) RT classified buildings, d) Fuzzy classified buildings

4.3. Accuracy Assessment Analysis

The building and non-building classes of the sample points were examined and served as standards to compare against the derived classes by computing the confusion matrix. Non-building class includes vegetation, roads, railway line and barren land. The classification result of NN, SVM, RT displayed in a confusion matrix as shown in the **Table 3, 4 and 5** respectively. The samples collected for each classification method also mentioned in the following tables.

Table 3. Error Matrix for the NN classified image

User Class/ Sample	Buildings	Non-Buildings	Sum
Buildings	115	12	131
Non-Buildings	16	162	174
Sum	131	174	
Producer's accuracy	0.8778	0.9310	
User's accuracy	0.8778	0.9310	
Overall accuracy = 0.9081	KC = 0.8126		

Table 4. Error Matrix for the SVM classified image

User Class/ Sample	Buildings	Non-Buildings	Sum
Buildings	109	14	123
Non-Buildings	16	92	108
Sum	125	106	
Producer's accuracy	0.872	0.868	
User's accuracy	0.8861	0.8518	
Overall accuracy = 0.8701	KC = 0.7388		

Table 5. Error Matrix for the RT classified image

User Class/ Sample	Buildings	Non-Buildings	Sum
Buildings	119	18	137
Non-Buildings	10	157	167
Sum	129	175	
Producer's accuracy	0.922	0.897	
User's accuracy	0.868	0.940	
Overall accuracy = 0.9078	KC = 0.813		

As showed from **Table 3,** overall accuracy of information extraction using NN classifier is 90.81% and kappa coefficient is 0.812. The overall accuracy of information extraction using SVM classifier is 87.01% and kappa coefficient is 0.7388 as depicted in **Table 4**. According to the **Table 5,** overall accuracy of classification of RT classifier is 90.78% and kappa coefficient is 0.813. The effect of overall classification is well except the misclassification few objects into other class. It is obvious that the nearest neighbour classifier can extract more information accurately than the other investigated classifiers, such as SVM and RT, by analysing the error matrix tables.

In area based accuracy measure, the seven different sorts of building footprints were digitised from HRS image and deployed as a reference for comparing with the extracted data. The building area in both reference image and the classified image is estimated in m^2 as shown in **Table 6** below. The accuracies were determined as percentages using the equations 1 and 2, for each extracted building in relation to the ground truth and the percentage of difference error also was calculated as shown in the below **Tables 7** and **8** respectively. The results revealed that the Fuzzy rule based classification provided a far higher overall accuracy percentage at 97.74%, followed by RF, NN, and SVM at 96.84%, 96.2%, and 96.12%, respectively.

Table 6. Area of reference buildings and extracted buildings

S. N	Building Type	Area (Sq. m)				
		NN	SVM	RF	Fuzzy	Reference
1	Blue Metal Sheet	2161.908	2161.908	2161.908	2161.908	2242.565
2	White sheet building	3886.902	3886.902	3886.902	3886.902	4000.925
3	Metal Roof	3921.292	3921.292	3921.292	3921.292	4021.529
4	Tin Roof	3826.364	3826.364	3826.364	3826.364	3827.17
5	White sheet building 2	1771.527	1771.527	1771.527	1771.527	1798.522
6	Concrete (with sheet)	4051.432	4085.768	3959.932	4231.509	4314.947
7	Fully concrete	3444.645	3373.237	3675.354	3675.354	3804.897

Table 7. Percentage accuracies of the extracted buildings

S. No	Building Type	Percentage Accuracy (%)			
		NN	SVM	RF	Fuzzy
1	Blue Metal Sheet	96.403	96.403	96.403	96.403
2	White sheet building	97.150	97.150	97.150	97.150
3	Metal Roof	97.507	97.507	97.507	97.507
4	Tin Roof	99.978	99.978	99.978	99.978
5	White sheet building 2	98.499	98.499	98.499	98.499
6	Concrete (with sheet)	93.892	94.688	91.772	98.066
7	Fully concrete	90.531	88.655	96.595	96.595
Overall Accuracy		96.280	96.126	96.843	97.742

Table 8. Difference error percentage of the extracted buildings

S. No	Building Type	Difference error (%)			
		NN	SVM	RF	Fuzzy
1	Blue Metal Sheet	-3.596	-3.596	-3.596	-3.596
2	White sheet building	-2.849	-2.849	-2.849	-2.849
3	Metal Roof	-2.492	-2.492	-2.492	-2.492
4	Tin Roof	-0.021	-0.021	-0.021	-0.021
5	White sheet building 2	-1.500	-1.500	-1.500	-1.500
6	Concrete (with sheet)	-6.107	-5.311	-8.227	-1.933
7	Fully concrete	-9.468	-11.344	-3.404	-3.404

In object based accuracy measure, the extracted buildings of rule based classification were used as it came out to be more accurate in area based accuracy assessment. The outcome of the object-based accuracy test is showed in **Table 9** below. The accuracy evaluation for the fuzzy rule-based extracted buildings is shown in **Figure 5**. The accuracy of extracted buildings achieves a greater accuracy rate with 88.24% completeness, 85.71% correctness, and 76.92% quality.

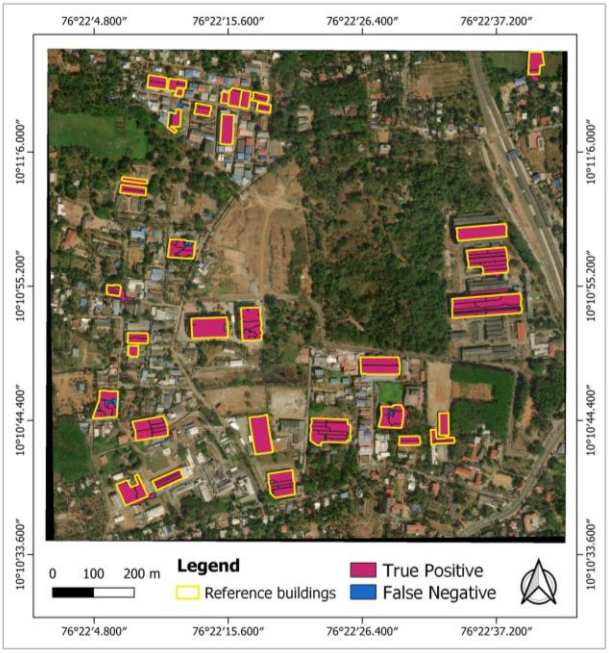

Figure 5. Object based accuracy assessment of fuzzy classified buildings

Table 9. Object based accuracies for the result of fuzzy rule based classification

Object Name	Total reference objects	Extracted objects (TP)	Falsely extracted (FP)	Not extracted objects (FN)	Completeness (%)	Correctness (%)	Quality
Extracted buildings	35	30	5	4	85.7142	88.2352	76.9230

The classification of the image using the Nearest Neighbour approach was more accurate than other methods that were taken into consideration, according to the results of the error matrix. The results indicated that the fuzzy rule set classification is providing more accurately identified building information by calculating the percentage accuracies and difference error with regard to the area-based accuracy measure. The extracted buildings from the same classification result are only taken into account in the object-based accuracy evaluation since the fuzzy membership function produces accurate results in area-based quantitative assessment. The ability of building feature detection has been computed using the percentages of completeness, accuracy, and quality. After comparing the outcomes of accuracy assessment, fuzzy rule based classification is shown to be the most ideal classification technique for extracting various building footprints.

5. Conclusion

In the present study, an HRS image is used to aid in the feature recognition and feature extraction of buildings from the complex industrial area. To detect and extract the buildings, multi-resolution segmentation has been offered, with the parameters of scale, shape, and compactness, user defined samples, and rule sets. The accurate building feature detection from different classification algorithms has also been verified using the estimated error matrix and the obtained area-based and object-based accuracy measures. According to the accuracy check findings, it is more accurate to detect buildings in an industrial region using object-based image classification. This methodology may be applied to high resolution satellite images. The buildings were extracted more precisely using NN classifier, with an overall accuracy of 90.81 % and a kappa coefficient of 0.812, according to the confusion matrix results. By adopting area-based accuracy measures, the competence of four supervised classifiers in classifying high-resolution images has been assessed and compared. The fuzzy rule based technique is the most effective way of extracting building footprints, and it has a 97.74 % overall accuracy. The fuzzy rule set's extracted buildings were put through an object-based accuracy test while taking ground reference data into account, yielding results of 88.24 % completeness, 85.71 % correctness, and 76.92 % quality.

Acknowledgement

The authors are thankful to Maxar’s Digital Globe for providing access to the high resolution data and to QGIS for allowing us to obtain the required Shapefiles used in the present study. Thanks are due to Director, IIRS for his encouragement and support.

Statement and Declarations:

There are no potential conflicts of interest for the authors to disclose.

References

[1] X. Fan, G. Nie, N. Gao, Y. Deng, J. An, and H. Li, "Building extraction from UAV remote sensing data based on photogrammetry method," *Int. Geosci. Remote Sens. Symp.*, vol. 2017-July, pp. 3317–3320, Dec. 2017, doi: 10.1109/IGARSS.2017.8127707.

[2] M. Awrangjeb, M. Ravanbakhsh, and C. S. Fraser, "Automatic detection of residential buildings using LIDAR data and multispectral imagery," *ISPRS J. Photogramm. Remote Sens.*, vol. 65, no. 5, pp. 457–467, Sep. 2010, doi: 10.1016/J.ISPRSJPRS.2010.06.001.

[3] A. Hamedianfar and H. Z. M. Shafri, "Detailed intra-urban mapping through transferable OBIA rule sets using WorldView-2 very-high-resolution satellite images," *http://dx.doi.org/10.1080/01431161.2015.1060645*, vol. 36, no. 13, pp. 3380–3396, Jul. 2015, doi: 10.1080/01431161.2015.1060645.

[4] A. Shukla and K. Jain, "Automatic extraction of urban land information from unmanned aerial vehicle (UAV) data," *Earth Sci. Informatics*, vol. 13, no. 4, pp. 1225–1236, 2020, doi: 10.1007/s12145-020-00498-x.

[5] T. R. Martha, N. Kerle, V. Jetten, C. J. van Westen, and K. V. Kumar, "Characterising spectral, spatial and morphometric properties of landslides for semi-automatic detection using object-oriented methods," *Geomorphology*, vol. 116, no. 1–2, pp. 24–36, Mar. 2010, doi: 10.1016/J.GEOMORPH.2009.10.004.

[6] S. Crommelinck, R. Bennett, M. Gerke, F. Nex, M. Y. Yang, and G. Vosselman, "Review of Automatic Feature Extraction from High-Resolution Optical Sensor Data for UAV-Based Cadastral Mapping," *Remote Sens. 2016, Vol. 8, Page 689*, vol. 8, no. 8, p. 689, Aug. 2016, doi: 10.3390/RS8080689.

[7] X. Jin and C. H. Davis, "Automated Building Extraction from High-Resolution Satellite Imagery in Urban Areas Using Structural, Contextual, and Spectral Information," *EURASIP J. Adv. Signal Process. 2005 200514*, vol. 2005, no. 14, pp. 1–11, Aug. 2005, doi: 10.1155/ASP.2005.2196.

[8] Y. Xiao, S. K. Lim, T. S. Tan, and S. C. Tay, "Feature extraction using very high resolution satellite imagery," *Int. Geosci. Remote Sens. Symp.*, vol. 3, pp. 2004–2007, 2004, doi: 10.1109/IGARSS.2004.1370741.

[9] T. Blaschke, C. Burnett, and A. Pekkarinen, "Image Segmentation Methods for Object-based Analysis and Classification," pp. 211–236, 2004, doi: 10.1007/978-1-4020-2560-0_12.

[10] J. Weickert, "Efficient image segmentation using partial differential equations and morphology," *Pattern Recognit.*, vol. 34, no. 9, pp. 1813–1824, Sep. 2001, doi: 10.1016/S0031-3203(00)00109-6.

[11] H. T. Li, H. Y. Gu, Y. S. Han, and J. H. Yang, "An efficient multi-scale segmentation for high- resolution remote sensing imagery based on statistical region merging and minimum heterogeneity rule," *2008 Int. Work. Earth Obs. Remote Sens. Appl. EORSA*, 2008, doi: 10.1109/EORSA.2008.4620351.

[12] I. Dronova *et al.*, "Landscape analysis of wetland plant functional types: The effects of image segmentation scale, vegetation classes and classification methods," *Remote Sens. Environ.*, vol. 127, pp. 357–369, Dec. 2012, doi: 10.1016/J.RSE.2012.09.018.

[13] M. Belgiu and L. D. Draˇgut, "Comparing supervised and unsupervised multiresolution segmentation approaches for extracting buildings from very high resolution imagery," 2014, doi: 10.1016/j.isprsjprs.2014.07.002.

[14] "Influence of point cloud density on the results of automated Object-Based building extraction from ALS data." http://repositori.uji.es/xmlui/handle/10234/98911 (accessed Aug. 08, 2022).

[15] I. Tomljenovic, D. Tiede, and T. Blaschke, "A building extraction approach for Airborne Laser Scanner data utilizing the Object Based Image Analysis paradigm," *Int. J. Appl. Earth Obs. Geoinf.*, vol. 52, pp. 137–148, Oct. 2016, doi: 10.1016/J.JAG.2016.06.007.

[16] "Open Data Program | Disaster Response Geospatial Analytics." https://www.maxar.com/open-data (accessed Aug. 01, 2022).

[17] G. Bongiovanni, L. Cinque, S. Levialdi, and A. Rosenfeld, “Image segmentation by a multiresolution approach,” *Pattern Recognit.*, vol. 26, no. 12, pp. 1845–1854, Dec. 1993, doi: 10.1016/0031-3203(93)90181-U.

[18] J. Torres-Sánchez, F. López-Granados, and J. M. Peña, “An automatic object-based method for optimal thresholding in UAV images: Application for vegetation detection in herbaceous crops,” *Comput. Electron. Agric.*, vol. 114, pp. 43–52, Jun. 2015, doi: 10.1016/J.COMPAG.2015.03.019.

[19] S. W. Myint and D. Stow, “An Object-Oriented Pattern Recognition Approach for Urban Classification,” *Urban Remote Sens. Monit. Synth. Model. Urban Environ.*, pp. 129–140, Apr. 2011, doi: 10.1002/9780470979563.CH9.

[20] B. W. Heumann, “An Object-Based Classification of Mangroves Using a Hybrid Decision Tree—Support Vector Machine Approach,” *Remote Sens. 2011, Vol. 3, Pages 2440-2460*, vol. 3, no. 11, pp. 2440–2460, Nov. 2011, doi: 10.3390/RS3112440.

[21] V. Lebourgeois *et al.*, “A Combined Random Forest and OBIA Classification Scheme for Mapping Smallholder Agriculture at Different Nomenclature Levels Using Multisource Data (Simulated Sentinel-2 Time Series, VHRS and DEM),” *Remote Sens. 2017, Vol. 9, Page 259*, vol. 9, no. 3, p. 259, Mar. 2017, doi: 10.3390/RS9030259.

[22] B. Aksoy and M. Ercanoglu, “Landslide identification and classification by object-based image analysis and fuzzy logic: An example from the Azdavay region (Kastamonu, Turkey),” *Comput. Geosci.*, vol. 38, no. 1, pp. 87–98, Jan. 2012, doi: 10.1016/J.CAGEO.2011.05.010.

[23] I. Lizarazo, “Accuracy assessment of object-based image classification: another STEP,” *https://doi.org/10.1080/01431161.2014.943328*, vol. 35, no. 16, pp. 6135–6156, Aug. 2014, doi: 10.1080/01431161.2014.943328.

[24] L. Cai, W. Shi, Z. Miao, and M. Hao, “Accuracy Assessment Measures for Object Extraction from Remote Sensing Images,” *Remote Sens. 2018, Vol. 10, Page 303*, vol. 10, no. 2, p. 303, Feb. 2018, doi: 10.3390/RS10020303.

[25] N. Sadhasivam, C. Dineshkumar, S. A. Rahaman, and A. Bhardwaj, “Object based Automatic Detection of Urban Buildings Using UAV Images,” *Proceedings of UASG 2019, Lecture Notes in Civil Engineering 51, Vol. 51, pp. 265-278, Feb. 2020,* https://doi.org/10.1007/978-3-030-37393-1_23 2019.

[26] X. Bai, H. Zhang, and J. Zhou, “VHR object detection based on structural feature extraction and query expansion,” *IEEE Trans. Geosci. Remote Sens.*, vol. 52, no. 10, pp. 6508–6520, 2014, doi: 10.1109/TGRS.2013.2296782.

[27] N. Laxmanrao Gavankar, & Sanjay, K. Ghosh, and S. K. Ghosh, “Object based building footprint detection from high resolution multispectral satellite image using K-means clustering algorithm and shape parameters,” *https://doi.org/10.1080/10106049.2018.1425736*, vol. 34, no. 6, pp. 626–643, May 2018, doi: 10.1080/10106049.2018.1425736.